ADVANCED BIOLOGY
www.advanced-bio.com

Spatiotemporal Control Over Multicellular Migration Using Green Light Reversible Cell–Cell Interactions

*Brice Nzigou Mombo, Brent M. Bijonowski, Samaneh Rasoulinejad, Marc Mueller, and Seraphine V. Wegner**

The regulation of cell–cell adhesions in space and time plays a crucial role in cell biology, especially in the coordination of multicellular behavior. Therefore, tools that allow for the modulation of cell–cell interactions with high precision are of great interest to a better understanding of their roles and building tissue-like structures. Herein, the green light-responsive protein CarH is expressed at the plasma membrane of cells as an artificial cell adhesion receptor, so that upon addition of its cofactor vitamin B_{12} specific cell–cell interactions form and lead to cell clustering in a concentration-dependent manner. Upon green light illumination, the CarH based cell–cell interactions disassemble and allow for their reversion with high spatiotemporal control. Moreover, these artificial cell–cell interactions impact cell migration, as observed in a wound-healing assay. When the cells interact with each other in the presence of vitamin B_{12} in the dark, the cells form on a solid front and migrate collectively; however, under green light illumination, individual cells migrate randomly out of the monolayer. Overall, the possibility of precisely controlling cell–cell interactions and regulating multicellular behavior is a potential pathway to gaining more insight into cell–cell interactions in biological processes.

Cell–cell adhesions are of fundamental importance in coordinating the behavior of cells in a multicellular context including cell migration, proliferation, and differentiation.[1] These contacts between cells transduce mechanical signals to neighboring cells and at the same time activate intracellular signaling cascades.[2] When and where cell–cell adhesions form is critical for cellular function. For example, the dynamic regulation of cell–cell interactions is an important parameter during morphogenesis and in maintaining tissue integrity, while it also regulates intercellular communication.[3] In contrast, the deregulation of cell–cell adhesions leads to the progression of cancer[1c] and subsequent metastasis.[4] Additionally, the control of cell–cell interactions is of interest in the field of bottom-up tissue-engineering, which aims to assemble cells as the basic unit into functional tissues.[5] Precise control in time and space over cell–cell interactions is required to successfully assemble appropriate multicellular architectures that resemble the in vivo structures and to control how cells work together within a tissue.

In recent years, many tools have been developed to control the formation and the disassembly of cell–cell interactions in a controlled manner and thereby have given insight into the role of cell–cell adhesions.[6] For instance, chemical modifications of the plasma membrane with bioorthogonal reactive functional groups[7] and specific noncovalent interaction partners[8] including complementary DNA strands,[9] biotin-streptavidin,[10] and supramolecular binding partners[11] result in the formation of chemical bonds between neighboring cells. However, in only a few examples, it is possible to reverse these cell–cell interactions once formed.[11] To overcome general concerns related to the chemical modification of the cell membrane (e.g., degradation over time, off-target cell toxicity), it is possible to regulate the expression and the activity of genetically encoded native cell–cell adhesion molecules such as cadherins[12] or artificial surface receptors.[1d,9b,6,12,13] These adhesions allow cells to not only just be brought together but in some cases also to transduce intracellular signals.[1e,12,14]

Photoregulation of cell–cell adhesions provides high spatiotemporal control, since light, as a stimulus, can be focused on the desired area and delivered at any given time. Using photocleavable nitrobenzyl[15] and switchable azobenzyl[14] chemical linkers, it has been shown possible to control cell–cell interactions with UV light.[11b,15,16] More recently, optogenetic tools for the regulation of cell–cell interactions with visible light have improved the biocompatibility,[13b,e] while also making it possible to dynamically and reversibly control cell–cell interactions between multiple cell types.[13b,e,16b,17] In these reports, photoswitchable proteins were expressed on the cell's plasma membrane as artificial adhesion molecules, which induced cell–cell interactions through the light-dependent dimerization of these proteins.[6] Depending on the photoswitchable proteins employed cell–cell adhesions between the same or different

B. Nzigou Mombo, Dr. B. M. Bijonowski, Prof. S. V. Wegner
Institute of Physiological Chemistry and Pathobiochemistry
University of Münster
Waldeyerstraße 15, Münster 48149, Germany
E-mail: wegnerse@exchange.wwu.de
Dr. S. Rasoulinejad, Dr. M. Mueller, Prof. S. V. Wegner
Max Planck Institute for Polymer Research
Ackermannweg 10, Mainz 55128, Germany
The ORCID identification number(s) for the author(s) of this article can be found under https://doi.org/10.1002/adbi.202000199.

DOI: 10.1002/adbi.202000199

types of cells were activated by either blue or red light and deactivated with different dynamics once the illumination was stopped.[6,13d,17] Photocontrol of cell–cell adhesions has allowed the programmed assembly of multicellular structures,[6a,b,16b] inducing interactions between T-cells and cancer cells for cancer immunotherapy[9b] and investigating mechanical coupling across cell–cell junctions.[16a]

In this study, we developed a novel biosynthetic cell–cell adhesion which forms in the presence of $AdoB_{12}$ (adenosylcobalamin, a form of vitamin B_{12}) and dissociates upon green light illumination using the protein CarH as an artificial cell–cell adhesion receptor. These green light cleavable cell–cell adhesions complement the existing repertoire of blue and red light switchable optogenetic cell–cell adhesions in terms of the illumination to which they respond. Unlike the previous examples,[6] green light illumination dissociates cell–cell adhesions rather than initiating association and induces irreversible changes to the cell–cell interactions with illumination such that existing cell–cell adhesions are retained even when illumination is stopped. Moreover, we demonstrated how these light-responsive artificial cell–cell adhesions alter collective cell behavior as observed in cell migration and provide spatiotemporal control over cell–cell adhesions.

In this study, we employed the green light-responsive protein CarH as an adhesion molecule to mediate cell–cell adhesions. The cobalamin binding domain of CarH derived from *Thermus thermophilus* is a monomer in the absence of its cofactor, $AdoB_{12}$, but forms a tetramer (a dimer of dimers) upon binding to $AdoB_{12}$. Exposure to blue or green light causes a ligand exchange at the $AdoB_{12}$ center in CarH, leading to a global conformational change in the protein and the disassembly of the CarH tetramer.[13b,16,18] The light responsiveness of CarH has previously been used for the optogenetic regulation of receptor signaling,[17] gene expression in cells,[19] as well as in material science to regulate mechanical properties and protein/cell release from hydrogels.[13a,20] It should be noted that these previous reports of CarH document that $AdoB_{12}$, green light illumination, and the CarH protein are highly biocompatible. In our design, we hypothesized that cells expressing the protein CarH on the plasma membrane will form cell–cell interactions in the presence of $AdoB_{12}$ as CarH tetramers assemble and that these interactions will be cleaved upon green light illumination, as the CarH tetramer photolyzes into its monomers (**Figure 1**a).

In this study, we expressed the cobalamin binding domain of CarH, referred to as CarH in the manuscript, on the plasma membrane by fusing it to a transmembrane anchoring domain (the C-terminal transmembrane anchoring domain of platelet-derived growth factor receptor) and an N-terminal secretion signal in the pDisplay vector (Figure S1, Supporting Information). It should be noted that the CarH expressed on the cell surface cannot link to the cytoskeleton as it does not contain the required intracellular domain. We transfected this construct into MDA-MB-231 cells, which do not form strong native cell–cell adhesions[6b,13c] and established a stable cell line, CarH-MDA, which expresses CarH on the plasma membrane. A single clone with high CarH expression was selected by flow cytometry (Figure S2, Supporting Information), and the protein expression was confirmed by confocal microscopy and quantitative flow cytometry measurements. Quantitative measurements

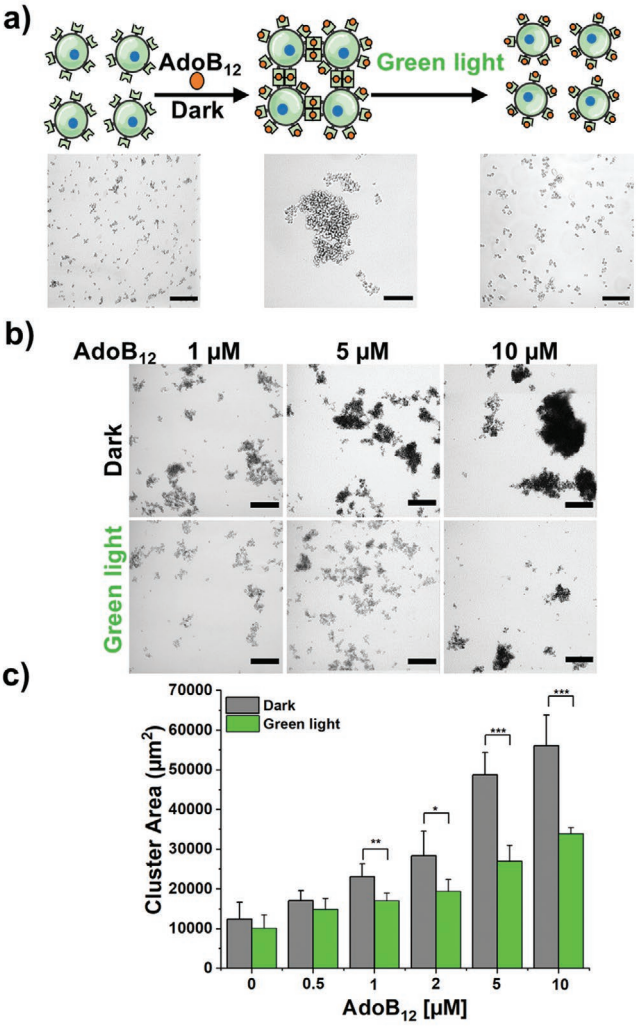

Figure 1. Green light responsive cell–cell interactions using CarH in the presence of $AdoB_{12}$. a) Schematic representation (upper line) and bright field microscopy images (lower line) of CarH-MDA cells, which express the green light responsive protein CarH at their plasma membrane. The CarH-MDA cells form cell–cell interactions in the dark in the presence of $AdoB_{12}$ (shown as orange circles, 5 μM) due to the multimerization of CarH. Under green light, the CarH dissociates into its monomers leading to the disassembly of the cell–cell interactions. Scale bars are 25 μm. b) Bright field images of CarH-MDA cells (5×10^4 cells mL^{-1}) in suspension in the dark and under green light in the presence of different concentrations of $AdoB_{12}$ incubated for 60 min at 30 rpm. Scale bars are 50 μm. c) Quantification of cell clustering in the dark and under green light in the presence of $AdoB_{12}$. All objects >5000 μm^2 were defined as cell clusters, a total sample area of 2.56 cm^2 was analyzed for each sample. Experiments were performed in biological duplicates with three technical replicates ($n = 6$). The error bars are the standard error of the mean, statistical significance was evaluated with unpaired Student's *t*-tests (two-tailed) and represented by *p*-values <0.05 (*), <0.01 (**), <0.001 (***).

showed ≈1×10^4 CarH photoreceptors per cell (Table S2, Supporting Information).

Next, we aimed to determine whether the CarH proteins can form intercellular linkages in the presence of $AdoB_{12}$ in the dark and whether these connections could be disassembled under green light illumination (Figure 1a). Indeed, when

we cultured CarH-MDA cells in suspension in the presence of 5 μM $AdoB_{12}$ in the dark, large multicellular clusters formed, but if the same cells were kept under green light illumination, only small, dispersed clusters were observable.

CarH requires its cofactor $AdoB_{12}$ to form a tetramer, and consequently, the number of active CarH proteins that can mediate cell–cell adhesion on the cell surface can be controlled through the $AdoB_{12}$ concentration in the media. To assess the role $AdoB_{12}$ plays in initiating CarH-MDA clustering, we incubated CarH-MDA cells in suspension, in the dark and under green light illumination (550 nm), for 1 h with different concentrations of $AdoB_{12}$ (0.5–10 μM) (Figure 1b). Quantification of the clustering using bright field microscopy (objects with a projected 2D area > 5000 μm^2 were defined as clusters),[6a,b] revealed that cells clustered significantly in the dark starting at concentrations of 1 μM $AdoB_{12}$ (23 084 μm^2) and resulted in significantly smaller clusters (17 065 μm^2) under green light illumination (Figure 1b,c, Figure S3, Supporting Information). Furthermore, there was a significant difference in the cell clustering depending on the concentration of cofactor used, with the projected area of the cell clusters in the dark doubling as the $AdoB_{12}$ concentration increased from 1 μM (23 084 μm^2) to 10 μM (56 105 μm^2). In parallel, the background clustering under green light increased as well with increasing $AdoB_{12}$ concentrations respectively from 1 μM (17 065 μm^2) to 10 μM (33 905 μm^2). On average, the projected cluster areas were 1.6-fold larger in the dark than under green light over the concentration range tested. At 0.5 μM $AdoB_{12}$, the difference between dark and green light was not significant, presumably due to insufficient loading of CarH with its cofactor. The herein observed concentration dependence is in agreement with the reported dissociation constant (K_D) of 250 nM between $AdoB_{12}$ and CarH, as determined by isothermal titration calorimetry.[18b] The results here showed that the majority of the surface-displayed CarH proteins have to be bound to the cofactor $AdoB_{12}$ for cell–cell adhesions to form.

Interestingly, the survival of cells in culture conditions requires only pM concentrations of vitamin B_{12}, while traditional cell culture media is supplemented with between 0 and 7.4 μM vitamin B_{12}. Many common cell culture media, including the herein used DMEM medium, do not contain exogenous vitamin B_{12}, and the addition of different concentrations of $AdoB_{12}$ allows for the modulation of CarH dependent cell–cell adhesions. While cell clustering was, as expected, less under green light than in the dark; we still observed an increase in the cell clustering under green light with increasing $AdoB_{12}$ concentrations. This finding illustrates that the formation/reformation of the CarH tetramers is faster than its dissociation even under green light illumination and could be explained in a few ways. For example, while the light-triggered ligand exchange at the $AdoB_{12}$ cofactor is known to be very fast (seconds), the disassembly of the CarH tetramer might be slower at the cell–cell contact sites due to high local concentrations of remaining CarH or excess $AdoB_{12}$, which might exchange with photolyzed $AdoB_{12}$ at which point it binds to CarH and reforms new CarH tetramers. Indeed, the reversion experiments shown below confirmed that the reversion of the cell–cell adhesions takes longer than 60 min of green light illumination.

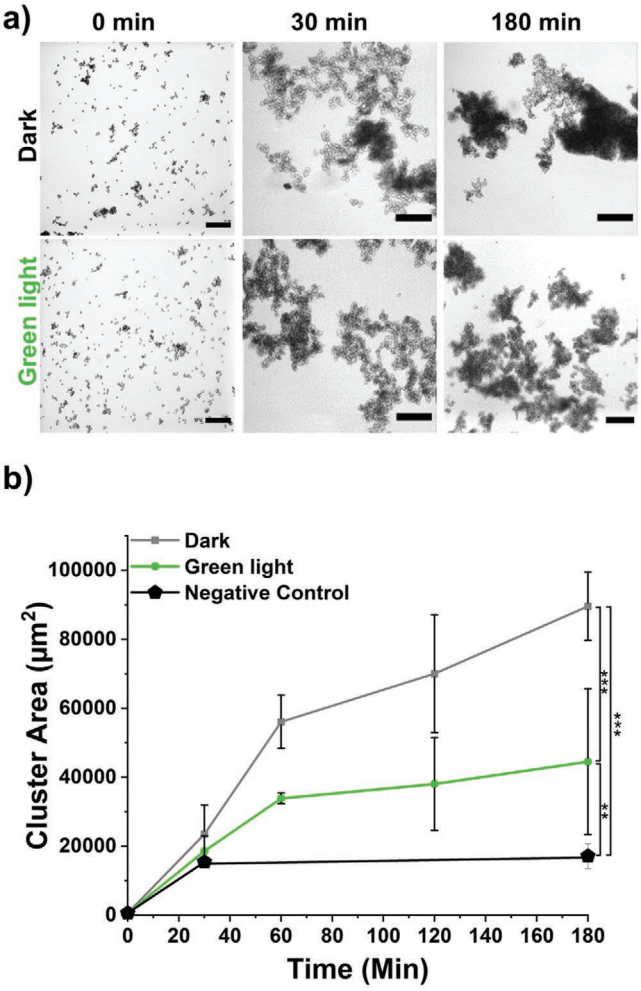

Figure 2. Time-dependent cell aggregation of CarH-MDA cells in the presence of 10 μM $AdoB_{12}$. a) Bright field images of CarH-MDA cells in suspension (5×10^4 cells mL^{-1}) in the presence of 10 μM $AdoB_{12}$ at different time points in the dark and under green light at 30 rpm. Scale bars are 50 μm. b) Quantification of the cell aggregation over time. Experiments were performed in biological duplicates with three technical replicates ($n = 6$). The error bars are the standard error of the mean, statistical significance was evaluated with unpaired Student's *t*-tests (two-tailed) and represented by *p*-values <0.05 (*), <0.01 (**), <0.001 (***).

Next, we evaluated the timeline for the assembly of multicellular clusters from CarH-MDA. For this purpose, we compared the size of clusters in the dark and under green light at different time points up to 180 min in the presence of 10 μM $AdoB_{12}$ (**Figure 2**). This concentration was chosen to ensure that most of the CarH proteins are loaded with the cofactor. At each time point, green light illumination resulted in significantly lower cell clustering than in the dark leading to a difference of 1.3-fold after 30 min and 2.0-fold after 180 min between the cluster area in the dark and green light. We also observed rapid cell clustering within the first 60 min for both dark and green illumination; however, afterward, the clusters only increased in size in the dark but not significantly under green light illumination. This is in line with the observation that the reversion of the cell–cell contacts presented below takes place only after

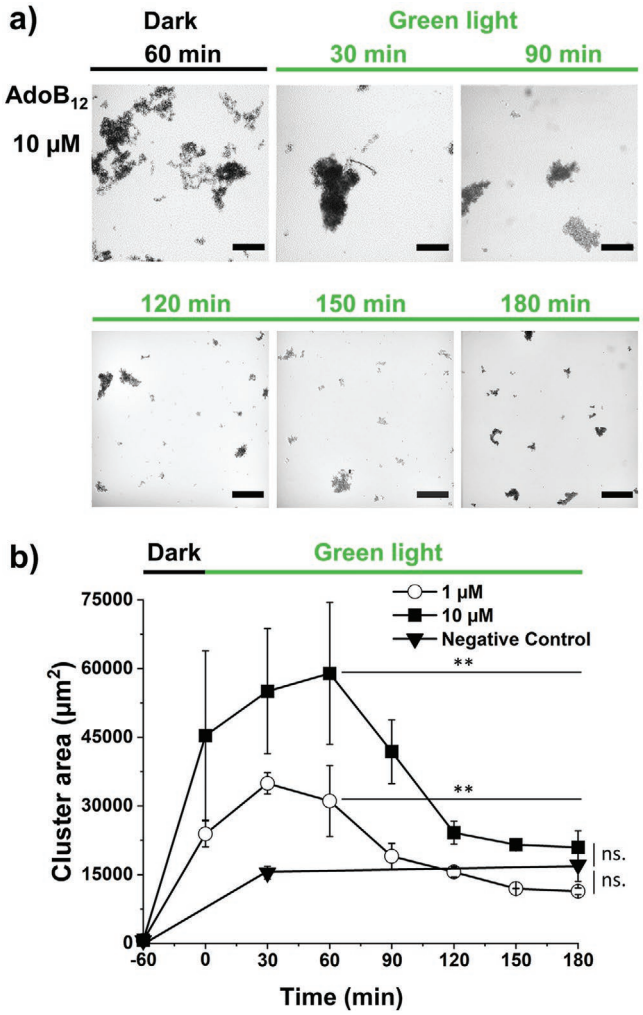

Figure 3. Reversibility of the cell–cell interactions under green light. a) Bright field images of CarH-MDA cells in suspension (5×10^4 cells mL^{-1}) in the presence of 1 or 10 μM $AdoB_{12}$ were kept in the dark for 60 min, before exposure to green light for up to 180 min. Scale bars are 50 μm. b) Quantification of the cell aggregation over time, where CarH cell–cell interactions formed between CarH-MDA cells were reversed under green light. Experiments were performed in biological duplicates with three technical replicates ($n = 6$). The error bars are the standard error of the mean, statistical significance was evaluated with unpaired Student's *t*-tests (two-tailed) and represented by *p*-values *ns*>0.05, <0.05 (*), <0.01 (**).

60 min under green light. A similar time-dependent analysis at low $AdoB_{12}$ concentrations (1 μM) showed that not only was the formed clusters smaller but also that clustering took longer (Figure S4, Supporting Information). The slower assembly of clusters at lower $AdoB_{12}$ concentrations is expected as fewer adhesion molecules at the cell surface are activated.

The reversibility of cell–cell interactions is an important aspect in multicellular structures, for instance, in cellular homing and tissue homeostasis.[21] To demonstrate that the cell–cell interactions in the CarH-MDA cells can be reversed at the desired point in time, we preincubated cells with different concentrations of $AdoB_{12}$ for 60 min in the dark and subsequently exposed them to increasing durations of green light up to 180 min (**Figure 3**a,b, Figure S5, Supporting Information). Both at low (1 μM) and high (10 μM) $AdoB_{12}$ concentrations, clusters continued to grow over the first 60 min following green light exposure before undergoing a reduction in cluster area (Figure 3a,b). After 120 min of green light illumination, the average cluster size decreased to the level observed for the negative control, which demonstrates the full reversion of the CarH based on the cell–cell adhesions. This slow reversion of the CarH mediated cell–cell interactions contrasts with the fast photoreaction of CarH at the molecular level. Additionally, it illustrates that the rate-limiting step is not the light response of the CarH protein, but another step, such as the separation of the cells. Similar trends of slower disassembly of the multicellular aggregates compared to the molecular reversion have been observed in other reports using photoswitchable proteins as artificial adhesion receptors.[6a,b] Moreover, as discussed above the multivalent protein–protein interactions between the cells and the exchange of the photolyzed $AdoB_{12}$ cofactor could be another reason for the continued clustering during the initial phase of green light illumination followed by the slow reversion of the cell–cell adhesions. The penetration of green light into the cluster is unlikely to be the limiting factor as the penetration depth of green light into human skin is reported to be 2.5 mm,[22] which is larger than the clusters formed herein.

Cell–cell adhesions are an important mechanism in coordinating multicellular behavior, one of the prime examples of which is collective cell migration.[23] During cellular migration, both mechanical and biochemical signals are transduced through cell–cell adhesions, which leads to enhanced coordination of cellular movement. In contrast, cells that lack canonical cell–cell adhesion molecules (e.g., cadherins), such as the herein used parent cell line MDA-MB-231, migrate independently from each other.[12] To evaluate if the artificial CarH based cell–cell interactions are sufficient to coordinate the migration of cells, which would normally migrate individually, we investigated the migration rate utilizing a wound-healing assay (**Figure 4**a). For this purpose, a confluent layer of CarH-MDA cells was wounded, and the migration rate of the wound edge was quantified in the dark and under green light in the presence (5 μM) or absence of $AdoB_{12}$ (Figure 4b). We observed that in the presence of both $AdoB_{12}$ in the dark, where the CarH based cell–cell interactions form, the cells formed a stable and coordinated front and migrated as a group forward. However, under green light illumination, individual cells were observed to migrate randomly into the open space out of the monolayer and the leading edge fragmented over time. Moreover, the wound front closed significantly faster in the dark than under green light. We observed a migration rate of 2.62 and 1.75 nm s^{-1} in the dark and under green light, respectively (Figure 4c). It should also be noted that unlike native cell–cell adhesions, which directly connect to the intracellular signaling via the actomyosin network, this is not the case for the CarH based artificial cell–cell interactions. Thus, physically connecting cells seems to be sufficient for cells to move together and even coordinate their movement resulting in a higher migration rate. Furthermore, this example showcases that these artificial cell–cell adhesions can be specifically activated, and underlie the construction of an important controllable model for coordinated tumor migration, metastasis, and general wound-healing.

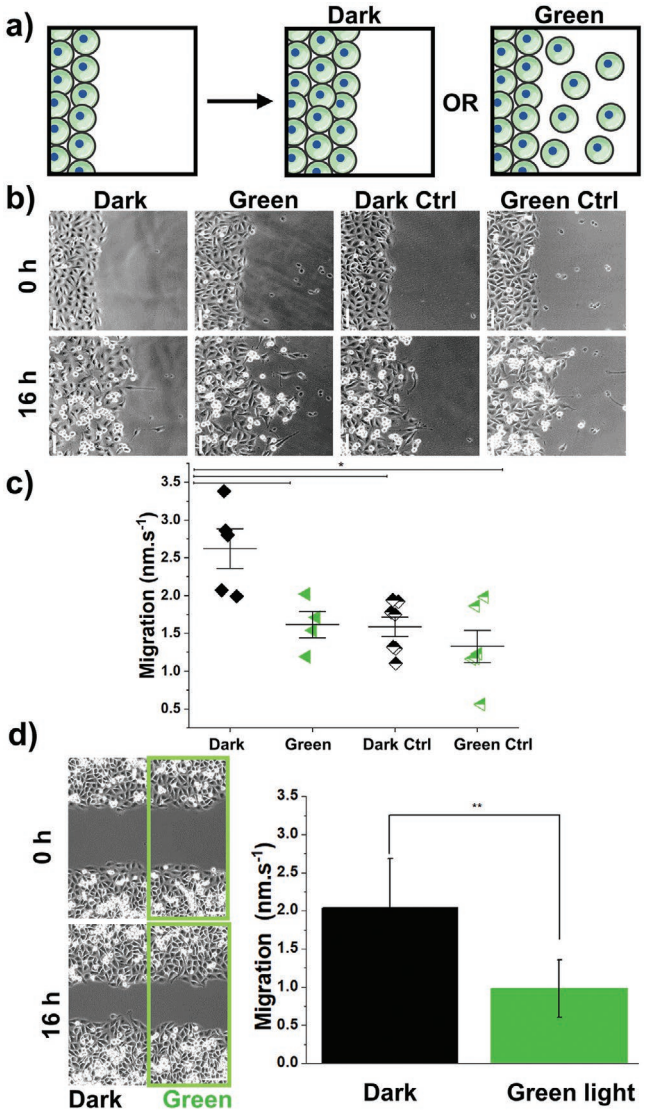

Figure 4. Cell migration of CarH-MDA cells. a) Schematic representation of CarH-MDA cells migrating into open space in the dark as a monolayer or under green light as individual cells. b) Bright field images of CarH-MDA cells migrating in a wound-healing assay in the presence (5 μM) or absence (Ctrl.) of $AdoB_{12}$ over 16 h. c) Quantification of migration rate of CarH-MDA cells for the conditions described in (b). d) Bright field images and quantification of CarH-MDA cells in the wound-healing assay where half of the field of view was illuminated with green light and the other side was kept in the dark. Scale bars in (b) and (d) are 100 μm. Experiments were performed in biological duplicate along with two technical replicates for each set ($n = 4$), the error bars are the standard error of the mean, statistical significance was evaluated using the one-way-ANOVA test and represented by p-values <0.05 (*), <0.01 (**).

Spatiotemporal photoregulation of cell–cell interactions allows for the side-by-side comparison of cellular migration of cells that are connected through the CarH adhesions and those that are not. For this purpose, we repeated the migration assay this time only illuminating half of the field of view with green light and keeping the other half in the dark (Figure 4d; Figure S6a and Movie S1, Supporting Information). The cell front of the wound in the unilluminated area migrated faster (2.05 nm s^{-1}) than in the illuminated area (0.95 nm s^{-1}). As a result, we observed that after 16 h, the CarH-MDA activated cells closed the wound more rapidly than the cells found in the illuminated portion of the sample. The analysis of individual cell trajectories at the wound edge and within the monolayer (Figure S6, Supporting Information) further corroborated these results. Both cells within the monolayer and at the wound edge migrated in a mostly linear fashion toward the wound in the dark (Figure S6b,d, Supporting Information); however migrated individually and randomly under green light (Figure S6c,e, Supporting Information). As a result, cells in the dark migrated further in the same amount of time than their counterparts in the green light. Thus, the linkage between cells CarH-MDA caused them to move together thereby coordinating their migration. Under green light, the cells migrated individually and randomly as a result of these connections being depleted. Garrod et al. showed a similar observation with the authors reporting that disruption of cellular adhesions such as desmosomes leads to decreased epidermal organization and wound healing rate.[24]

In summary, the herein established surface expression of CarH at the plasma membrane enables the optogenetic regulation of cell–cell interactions. In particular, stable cell–cell interactions form in the presence of $AdoB_{12}$, which can be fully dissociated upon green light illumination. Notably, the extent of cell–cell interactions depends on the concentration of the cofactor $AdoB_{12}$ thus allowing for the tuning of multicellular clusters. Unlike previous optogenetic cell–cell interactions, which form upon blue or red light illumination and reverse in the dark,[6a–c] the CarH based interactions irreversibly disassemble upon illumination and are stable in the dark. Thus, CarH based cell–cell interactions do not require constant illumination, and once the desired cell–cell interactions are established, they are maintained until disrupted with green light illumination. This feature is particularly important in the context of bottom-up tissue engineering, where the CarH based cell–cell interactions would allow for the maintenance of multicellular tissue-like structures in the absence of light. Moreover, herein we have demonstrated for the first time that artificial cell–cell adhesions can establish collective cellular migration in cells that would otherwise migrate individually. Most interestingly, we have shown that the physical contact between cells, without a direct link to the intracellular signaling, is sufficient for this coordinated action which leads to faster cellular migration. Overall, we believe that the herein established CarH based artificial cell–cell adhesions are a great tool for investigating the role of cell–cell adhesions in biology and the assembly of precise multicellular structures.

Supporting Information

Supporting Information is available from the Wiley Online Library or from the author.

Acknowledgements

This work was funded by the European Research Council ERC Starting Grant ARTIST (# 757593). The authors would like to thank Dr. Stefanie Möckel and Dr. Jesús Gil Pulido at the Flow Cytometry Core Facility

(FCCF) at the Institute of Molecular Biology (IMB) in Mainz, Germany for their support with FACS measurements.

Conflict of Interest

The authors declare no conflict of interest.

Keywords

$AdoB_{12}$, CarH, cell–cell interactions, migration, reversibility

Received: August 4, 2020
Revised: November 22, 2020
Published online: January 14, 2021

[1] a) B. M. Gumbiner, *Nat. Rev. Mol. Cell Biol.* **2005**, *6*, 622; b) S. Lamouille, J. Xu, R. Derynck, *Nat. Rev. Mol. Cell Biol.* **2014**, *15*, 178; c) G. Moreno-Bueno, H. Peinado, P. Molina, D. Olmeda, E. Cubillo, V. Santos, J. Palacios, F. Portillo, A. Cano, *Nat. Protoc.* **2009**, *4*, 1591; d) J. W. Nichol, A. Khademhosseini, *Soft Matter* **2009**, *5*, 1312; e) M. S. Steinberg, *Science* **1963**, *141*, 401.

[2] W. Engl, B. Arasi, L. L. Yap, J. P. Thiery, V. Viasnoff, *Nat. Cell Biol.* **2014**, *16*, 584.

[3] Z. Cesarz, J. L. Funnell, J. Guan, K. Tamama, *Stem Cells Dev.* **2016**, *25*, 622.

[4] R. Kalluri, R. A. Weinberg, *J. Clin. Invest.* **2009**, *119*, 1420.

[5] a) D. L. Elbert, *Curr. Opin. Biotechnol.* **2011**, *22*, 674; b) S. Toda, L. R. Blauch, S. K. Y. Tang, L. Morsut, W. A. Lim, *Science* **2018**, *361*, 156.

[6] a) M. Mueller, S. Rasoulinejad, S. Garg, S. V. Wegner, *Nano Lett.* **2019**, *20*, 2257; b) S. Rasoulinejad, M. Mueller, B. Nzigou Mombo, S. V. Wegner, *ACS Synth. Biol.* **2020**, *9*, 2076; c) S. G. Yüz, S. Rasoulinejad, M. Mueller, A. E. Wegner, S. V. Wegner, *Adv. Biosyst.* **2019**, *3*, 1800310; d) S. G. Yüz, J. Ricken, S. V. Wegner, *Adv. Sci.* **2018**, *5*, 1800446.

[7] a) D. Dutta, A. Pulsipher, W. Luo, M. N. Yousaf, *J. Am. Chem. Soc.* **2011**, *133*, 8704; b) H. Koo, M. Choi, E. Kim, S. K. Hahn, R. Weissleder, S. H. Yun, *Small* **2015**, *11*, 6458.

[8] K. Gabrielse, A. Gangar, N. Kumar, J. C. Lee, A. Fegan, J. J. Shen, Q. Li, D. Vallera, C. R. Wagner, *Angew. Chem., Int. Ed.* **2014**, *53*, 5112.

[9] a) Z. J. Gartner, C. R. Bertozzi, *Proc. Natl. Acad. Sci. USA* **2009**, *106*, 4606; b) Z. Ge, J. Liu, L. Guo, G. Yao, Q. Li, L. Wang, J. Li, C. Fan, *J. Am. Chem. Soc.* **2020**, *142*, 8800.

[10] P. A. De Bank, Q. Hou, R. M. Warner, I. V. Wood, B. E. Ali, S. Macneil, D. A. Kendall, B. Kellam, K. M. Shakesheff, L. D. Buttery, *Biotechnol. Bioeng.* **2007**, *97*, 1617.

[11] a) P. Shi, N. Zhao, J. Lai, J. Coyne, E. R. Gaddes, Y. Wang, *Angew. Chem., Int. Ed.* **2018**, *57*, 6800; b) P. Shi, E. Ju, Z. Yan, N. Gao, J. Wang, J. Hou, Y. Zhang, J. Ren, X. Qu, *Nat. Commun.* **2016**, *7*, 13088.

[12] D. Ollech, T. Pflästerer, A. Shellard, C. Zambarda, J. P. Spatz, P. Marcq, R. Mayor, R. Wombacher, E. A. Cavalcanti-Adam, *Nat. Commun.* **2020**, *11*, 472.

[13] a) R. Wang, Z. Yang, J. Luo, I. M. Hsing, F. Sun, *Proc. Natl. Acad. Sci. USA* **2017**, *114*, 5912; b) L. Klewer, Y.-W. Wu, *Chem. - Eur. J.* **2019**, *25*, 12452; c) M. T. Nieman, R. S. Prudoff, K. R. Johnson, M. J. Wheelock, *J. Cell Biol.* **1999**, *147*, 631; d) K. Muller, W. Weber, *Mol. BioSyst.* **2013**, *9*, 596; e) B. R. Rost, F. Schneider-Warme, D. Schmitz, P. Hegemann, *Neuron* **2017**, *96*, 572; f) K. Gabrielse, A. Gangar, N. Kumar, J. C. Lee, A. Fegan, J. J. Shen, Q. Li, D. Vallera, C. R. Wagner, *Angew. Chem., Int. Ed. Engl.* **2014**, *53*, 5112.

[14] L. Morsut, K. T. Roybal, X. Xiong, R. M. Gordley, S. M. Coyle, M. Thomson, W. A. Lim, *Cell* **2016**, *164*, 780.

[15] W. Luo, A. Pulsipher, D. Dutta, B. M. Lamb, M. N. Yousaf, *Sci. Rep.* **2014**, *4*, 6313.

[16] a) D. B. Konrad, G. Savasci, L. Allmendinger, D. Trauner, C. Ochsenfeld, A. M. Ali, *J. Am. Chem. Soc.* **2020**, *142*, 6538; b) N. S. Selden, M. E. Todhunter, N. Y. Jee, J. S. Liu, K. E. Broaders, Z. J. Gartner, *J. Am. Chem. Soc.* **2012**, *134*, 765.

[17] S. Kainrath, M. Stadler, E. Reichhart, M. Distel, H. Janovjak, *Angew. Chem., Int. Ed.* **2017**, *56*, 4608.

[18] a) J. M. Ortiz-Guerrero, M. C. Polanco, F. J. Murillo, S. Padmanabhan, M. Elias-Arnanz, *Proc. Natl. Acad. Sci. USA* **2011**, *108*, 7565; b) R. J. Kutta, S. J. O. Hardman, L. O. Johannissen, B. Bellina, H. L. Messiha, J. M. Ortiz-Guerrero, M. Elías-Arnanz, S. Padmanabhan, P. Barran, N. S. Scrutton, A. R. Jones, *Nat. Commun.* **2015**, *6*, 7907; c) M. Jost, J. Fernandez-Zapata, M. C. Polanco, J. M. Ortiz-Guerrero, P. Y. Chen, G. Kang, S. Padmanabhan, M. Elias-Arnanz, C. L. Drennan, *Nature* **2015**, *526*, 536; d) M. C. Perez-Marin, S. Padmanabhan, M. C. Polanco, F. J. Murillo, M. Elias-Arnanz, *Mol. Microbiol.* **2008**, *67*, 804.

[19] C. Chatelle, R. Ochoa-Fernandez, R. Engesser, N. Schneider, H. M. Beyer, A. R. Jones, J. Timmer, M. D. Zurbriggen, W. Weber, *ACS Synth. Biol.* **2018**, *7*, 1349.

[20] T.-T. Li, X. Cen, H.-T. Ren, F. Sun, Q. Lin, C.-W. Lou, J.-H. Lin, *Polymers* **2019**, *11*, 1307.

[21] J. D. Humphrey, E. R. Dufresne, M. A. Schwartz, *Nat. Rev. Mol. Cell Biol.* **2014**, *15*, 802.

[22] C. Ash, M. Dubec, K. Donne, T. Bashford, *Lasers Med. Sci.* **2017**, *32*, 1909.

[23] J. H. Venhuizen, M. M. Zegers, *Cold Spring Harbor Perspect. Biol.* **2017**, *9*, a027854.

[24] D. R. Garrod, M. Y. Berika, W. F. Bardsley, D. Holmes, L. Tabernero, *J. Cell Sci.* **2005**, *118*, 5743.